#### ORIGINAL ARTICLE



# Meiotic pairing and double-strand break formation along the heteromorphic threespine stickleback sex chromosomes

Shivangi Nath · Lucille A. Welch · Mary K. Flanagan · Michael A. White

Received: 14 February 2022 / Revised: 2 May 2022 / Accepted: 4 May 2022 © The Author(s), under exclusive licence to Springer Nature B.V. 2022

Abstract Double-strand break repair during meiosis is normally achieved using the homologous chromosome as a repair template. Heteromorphic sex chromosomes share little sequence homology, presenting unique challenges to the repair of doublestrand breaks. Our understanding of how heteromorphic sex chromosomes behave during meiosis has been focused on ancient sex chromosomes, where the X and Y differ markedly in overall structure and gene content. It remains unclear how more recently evolved sex chromosomes that share considerably more sequence homology with one another pair and form double-strand breaks. One possibility is barriers to pairing evolve rapidly. Alternatively, recently evolved sex chromosomes may exhibit pairing and double-strand break repair that more closely resembles that of their autosomal ancestors. Here, we use the recently evolved X and Y chromosomes of the threespine stickleback fish (Gasterosteus aculeatus) to study patterns of pairing and double-stranded break formation using molecular cytogenetics. We found that the sex chromosomes of threespine stickleback fish did not pair exclusively in the pseudoautosomal region. Instead, the chromosomes fully paired in a non-homologous fashion. To achieve this, the X chromosome underwent synaptic adjustment during pachytene to match the axis length of the Y chromosome. Double-strand break formation and repair rate also matched that of the autosomes. Our results highlight that recently evolved sex chromosomes exhibit meiotic behavior that is reminiscent of autosomes and argues for further work to identify the homologous templates that are used to repair double-strand breaks on the X and Y chromosomes.

**Keywords** Meiosis · sex chromosomes · threespine stickleback · double-strand breaks · synaptic adjustment

### **Abbreviations**

**DSB** Double-strand breaks

**FISH** Fluorescent in situ hybridization

Isocitrate dehydrogenase Idh RAD51 recombinase

RAD51

Structural maintenance of chromosomes 3 SMC3

# Introduction

Meiosis is a specialized form of cellular division that results in the formation of haploid gametes. In order to produce functional gametes, the chromosomes have to segregate properly such that each gamete receives only one copy of each homologous chromosome pair. If chromosomes fail to pair and segregate correctly, severe meiotic errors can result (reviewed in Hassold

Responsible Editor: Beth Sullivan.

S. Nath  $\cdot$  L. A. Welch  $\cdot$  M. K. Flanagan  $\cdot$  M. A. White  $(\boxtimes)$ Department of Genetics, University of Georgia, 120 Green St, Athens, GA 30602, USA e-mail: whitem@uga.edu

Published online: 30 May 2022



and Hunt 2001). In many species, pairing is initiated by the formation of double strand breaks (DSBs) (Baudat et al. 2000; Romanienko and Camerini-Otero 2000; Grelon et al. 2001) that are then repaired using intact sequence from the homologous chromosome as a template. Heteromorphic sex chromosomes pairs (X/Y or Z/W) present unique challenges in terms of pairing and DSB repair during meiosis due to their overall lack of sequence homology between the chromosomes available for DSB repair (Page et al. 2005, 2006; Fuente et al. 2007, 2012; Kauppi et al. 2011, 2012; Checchi and Engebrecht 2011; Borodin et al. 2011; Guioli et al. 2012; Lu and Yu 2015; Dumont et al. 2018).

Our understanding of how heteromorphic sex chromosomes pair and how double-strand break initiation and repair occurs has largely been informed by detailed studies of the ancient X and Y chromosomes of mammals (Fuente et al. 2007, 2012; Kauppi et al. 2011, 2012; Borodin et al. 2011; Dumont et al. 2018) and the ancient Z and W chromosome of birds (Schoenmakers et al. 2009; Guioli et al. 2012). Heteromorphic sex chromosomes share a region of complete homology (the pseudoautosomal region) that undergoes an obligate crossover each meiosis (Burgovne 1982; Rouyer et al. 1986; Soriano et al. 1987; Hassold et al. 1991). During meiosis, the sex chromosomes of most mammals exhibit delayed pairing and only synapse within the pseudoautosomal region, while the sex-limited, non-homologous regions remain largely unpaired (Rasmussen and Holm 1978; Burgoyne 1982; Chandley et al. 1984; Kauppi et al. 2011; Federici et al. 2015). Double-strand breaks continue to form within the unsynapsed axial element of the X or Z chromosome (Ashley et al. 1995; Moens et al. 1997; Barlow et al. 1997; Mahadevaiah et al. 2001; Lange et al. 2016; Enguita-Marruedo et al. 2019), whereas they are largely suppressed on the axial element of the sex-limited chromosome (Moens et al. 1997; Lange et al. 2016). The double-strand breaks that do form within the non-homologous region exhibit delayed repair relative to the autosomes and are primarily repaired through homologous exchange with the sister chromatid or via non-homologous end joining (Checchi and Engebrecht 2011). In birds, the lack of sequence homology between much of the Z and W chromosome has resulted in error prone synapsing, with a complete failure of pairing in nearly a quarter of oocytes (Guioli et al. 2012).

Although it is clear that highly degenerate sex chromosomes must navigate meiosis in a manner unique from autosomes, it is unknown how quickly these modifications are established following the evolution of sex chromosomes. Comparisons with recently evolved sex chromosomes are needed to understand how pairing and double-strand break repair are altered from their autosomal ancestors. Young sex chromosomes share higher sequence homology with one another compared to older sex chromosomes that have accumulated mutations over a longer time period (reviewed in Bachtrog 2013). This raises the possibility that younger sex chromosomes may exhibit more extensive pairing depending on the amount of sequence and structural divergence outside of the pseudoautosomal region. In addition, doublestrand breaks may form and be repaired at rates that more closely resemble autosomes than that observed on ancient sex chromosomes. If the repair of doublestrand breaks occurs more often between the X and Y or Z and W through non-crossover gene conversion, these breaks could be repaired earlier in meiosis before the barrier to sister chromatid and non-homologous end joining repair is lifted (Inagaki et al. 2010; Enguita-Marruedo et al. 2019).

Threespine sticklebacks (Gasterosteus aculeatus) are a useful species to study the behavior of recently evolved sex chromosomes during meiosis. They have an X and Y sex chromosome system which evolved only approximately 22 million years ago (Peichel et al. 2020), compared to the ~ 180 million-year-old Y chromosome of mammals (Bellott et al. 2014; Cortez et al. 2014) or the ~ 100 million-year-old W chromosome of birds (Zhou et al. 2014). Crossing over between the X and Y chromosomes is suppressed across most of the chromosome pair outside of a 2.50-Mb pseudoautosomal region (Roesti et al. 2013). The sex-determining region coincides with three major inversions between the X and Y, which form three separate evolutionary strata (Ross et al. 2009; Peichel et al. 2020). Despite the structural differences between the X and Y, meiotic nuclei isolated from a single population indicated the sex chromosomes may synapse fully in males along their length (Cuñado et al. 2002). However, due to limited sample sizes, it is unknown whether the X and Y synapse fully in a majority of meiocytes or if full pairing is mostly achieved only in the pseudoautosomal region, similar to species with ancient sex chromosomes (Solari 1974). In addition, the overall timing



and rate of meiotic double-strand break formation and repair is unknown between recently derived X and Y chromosomes. Synonymous sequence divergence is an order of magnitude lower in the youngest strata of the threespine stickleback X and Y chromosomes compared to the youngest strata of the human X and Y (Peichel et al. 2020). Threespine stickleback fish therefore present an ideal opportunity to explore whether double-strand breaks on young sex chromosomes exhibit repair dynamics that more closely resemble that of their autosomal ancestral counterparts.

Here, we use molecular cytogenetics to closely examine pairing and double-strand break formation of autosomes and sex chromosomes during male meiosis. Contrary to what has been observed in species with ancient sex chromosomes, we found the more recently evolved sex chromosomes of threespine stickleback fish fully pair and repair double-strand breaks at the same rate as autosomes.

#### Materials and methods

#### Ethics statement

All procedures using threespine stickleback fish were approved by the University of Georgia Animal Care and Use Committee (protocol A2018 10–003-A8).

# Preparation of meiotic nuclei

Chromosome spreads were prepared using a modified protocol developed for zebrafish (Blokhina et al. 2019). We targeted threespine stickleback fish that were approximately 5 to 8 months after hatching (standard length approximately 5.4 cm), when testes were actively undergoing meiosis (Naftaly et al. 2021). Stickleback fish undergo synchronized spermatogenesis and testes of juvenile fish are enriched for similarly staged meiocytes (Craig-Bennett 1931; Borg 1982). Whole testes were dissected and macerated using a Dounce homogenizer in a volume of 200 µL PBS buffer. The cell suspension was centrifuged for 5 min at  $200 \times g$  and the pellet was resuspended in 200 µL of 100 mM sucrose. The cell suspension was incubated for 5 min at room temperature. In total, 20 µL of the suspension was pipetted across a clear slide and then 100 µL of fixative (1% paraformaldehyde with 0.15% Triton-X 100) was added and the slide was left overnight in a humid chamber. The slides were washed the next day in  $1 \times PBS$  three times for 15, 10, and 5 min and then stored at -20 °C.

### Immunofluorescence of SMC3 and RAD51

We adapted an immunofluorescence protocol from Dumont and Payseur (2011). The spreads were permeabilized by pipetting 1.5 mL of permeabilization solution (1×PBS, 1 mM EDTA, and 1% TritonX-100) on the slide and incubating for 20 min at room temperature (Dawe et al. 2018). The slides were then blocked by adding 1.5 mL of 1 × antibody dilution buffer and incubating for 20 min at room temperature. After blocking, the slides were incubated with diluted primary antibodies (1:100 anti-SMC3, Abcam ab9263; 1:40 anti-RAD51, Invitrogen MA5-14419) in 40 μL of 1×PBS per slide. The slides were sealed with a coverslip and rubber cement and then incubated at 4 °C overnight. After the primary incubation coverslip was removed, the slides were blocked with 1 x antibody dilution buffer for 20 min. Secondary antibodies (goat antirabbit, Abcam ab150077, ab150080, and ab150079; goat anti-mouse, Abcam ab150113) were applied at the same dilution as the primary antibodies, sealed with a coverslip and rubber cement, and incubated for 2 h at 37 °C. After the secondary incubation, the slides were washed in  $1 \times PBS$  three times (15 min, 5 min, and 5 min). The slides were sealed with a coverslip and Vectashield Antifade Mounting Media (Vector Labs).

#### Staging of nuclei

The spreads were staged to substages of prophase I by the following criteria: leptotene spreads were defined by small SMC3 stretches forming along chromosomes; zygotene was defined by long SMC3 stretches covering entire chromosomes undergoing synapsis, although not all homologs were fully paired (the number of chromosomes at this stage ranged from 42 unpaired homologs to two unpaired homologs); and pachytene was characterized as all homologs being paired, with a total diploid chromosome count of 21.



# Fluorescence in situ hybridization

The X and Y chromosomes were distinguished using the previously characterized sex-linked bacterial artificial chromosomes (BAC) clone, 101E08 (*Idh*, isocitrate dehydrogenase) from the CHORI-213 library (Peichel et al. 2004; Ross and Peichel 2008). The BAC containing Idh was extracted from 200-mL bacterial cultures using the NucleoBond Xtra Midi kit (Takara Bio). The fluorescence in situ hybridization (FISH) probes were made using a Vysis Nick Translation Kit (Abbott Molecular), following the manufacturer's instructions, except for the addition of 2 µg of input DNA for each reaction, rather than the 1 µg suggested. The reagents were mixed and incubated for 16 h at 15 °C, followed by inactivation for 15 min at 7 °C. After nick translation, 10 µL of each probe was precipitated with 1 µL of salmon sperm DNA (ThermoFisher Scientific), 30.3 µL of 100% ethanol, and 1.1 µL of 3 M sodium acetate, over 15 min at room temperature in the dark. The probes were then centrifuged for 30 min at 4 °C at 12,000 rpm. The supernatant was discarded, and the pellet was left to dry at room temperature for 15 min. The pellet was then reconstituted in 2 µL of TE (pH 8.0) and 8 µL of hybridization buffer (5 mL 100% formamide, 1 mL 20×SSC pH 7.0, 2 mL 50% dextran sulfate). The FISH probes were hybridized to the same slides used for immunofluorescence. The slides were incubated with 2×SSC at 75 °C for 5 min and then treated with denaturing solution (2×SSC, 70% formamide) for 2 min. The slides were then passed through an ethanol series (70%, 85%, and 100%) for 2 min each and dried in a slanted position for 10 min. In total, 10 µL of the precipitated and reconstituted probe was put on the slide and sealed with a coverslip and rubber cement. The slides were incubated overnight at 37 °C and washed the next day three times at 45 °C in  $2 \times SSC/50\%$  formamide (pH 7.0), followed by three washes at 45 °C in 2×SSC. Each wash was 5 min each. After drying, the slides were mounted with Vectashield Antifade Mounting Media (Vector Laboratories). All slides were imaged using a Leica DM6000 B upright microscope at × 63 magnification with DAPI, TRITC, Alexa633, and FITC filter sets. All images were captured using a Hamamatsu ORCA-ER digital camera.

# Quantification of synaptic adjustment

Synaptic adjustment was only measured in nuclei where the sex chromosomes were fully paired and there were two clear *Idh* foci, one from the X chromosome and one from the Y chromosome. Sex chromosomes from pachytene and zygotene stages from four different males were categorized into two different conformations. In one conformation, the X chromosome *Idh* was located at the center of the paired chromosomes axis and the Y chromosome *Idh* was at an intermediate position between the center *Idh* and the chromosome *Idh* was located centrally and the Y chromosome *Idh* was at the very end of the paired chromosome *Idh* was at the very end of the paired chromosome axis.

We examined whether the size of chromatin loops extending from the synaptonemal complex axis differed among the conformations by measuring the total width of the X chromosome and Y chromosome *Idh* marker signals extending from SMC3 using ImageJ (https://imagej.nih.gov/ij/). The freehand tool was used to draw a line connecting the two ends of each *Idh* probe that extended from the chromosome axis. The length of each line was measured in pixels and converted to microns by multiplying by a factor of 0.13 μm/pixel.

For both conformations, the number of RAD51 foci was also counted. To analyze the distribution of RAD51 foci across the sex chromosomes, the length of each chromosome was measured using ImageJ and then divided into five equal parts based on the total length of the SMC3 axis. The number of DSBs were then recorded in each interval. A total of 420 autosomes and 47 sex chromosomes from spreads in zygotene/pachytene were counted.

## Double-strand break counting and normalization

For each meiotic nucleus, the total number of RAD51 foci were counted on the autosomes and the sex chromosomes. The counts were repeated three times and the average was used. The counting was conducted blinded in respect to the substage of prophase. The density of DSBs per Mb was calculated by dividing the genome-wide counts by the diploid genome size of 910.06 Mb, while the number of DSBs on the sex chromosomes was divided by 38.60 Mb (the total size of the X chromosome and Y chromosome combined).



Data availability

The data underlying this article are available in the article.

#### Results

The threespine stickleback X and Y chromosomes pair non-homologously during meiosis

Outside of the 2.50-Mb pseudoautosomal region, the three evolutionary strata within the non-crossover region of the sex chromosomes have varied degrees of sequence degeneration. Synonymous site nucleotide divergence is highest within the oldest stratum (stratum 1; 15.5%), whereas the two younger strata are considerably more similar at the sequence level between the X and Y (stratum 2: 4.2% synonymous site nucleotide divergence; stratum 3: 3.3% synonymous site nucleotide divergence) (Peichel et al. 2020). In addition to having altered orientations between the X and Y chromosomes, the three inverted strata also have accumulated numerous duplications and deletions, resulting in length variation between the X and Y (stratum 1: 8.08 Mb X, 4.33 Mb Y; stratum 2: 4.39 Mb X, 5.00 Mb Y; stratum 3: 5.61 Mb X, 6.19 Mb Y) (Fig. 1) (Peichel et al. 2020). Combined, sequence order and orientation between the X and Y chromosomes outside of the pseudoautosomal region have been disrupted, suggesting the X and Y chromosomes may not fully pair during meiosis, similar to the ancient sex chromosomes of mammals (Rasmussen and Holm 1978; Burgoyne 1982; Chandley et al. 1984; Kauppi et al. 2011; Federici et al. 2015). To observe how the X and Y chromosomes pair, we used a well-characterized cytogenetic marker (Idh) to differentiate the chromosomes throughout prophase I (Idh is located in the middle of the X chromosome at 11.5 Mb and at the end of the Y chromosome at 18.02 Mb, opposite of the pseudoautosomal region) (Ross et al. 2009; Peichel et al. 2020). Using this marker as a probe, we found that the X and Y chromosomes synapsed fully during late zygotene and pachytene, when synapsis was also complete on the autosomes (Fig. 1). We found the X-linked *Idh* (X-Idh) marker was in the middle of the sex chromosome pair while the *Idh* marker on the Y chromosome (Y-Idh) was located further distal from the pseudoautosomal region on the synapsed chromosome pair (full synapsis was observed in 50 out of 51 nuclei). Given the large-scale structural rearrangements between the sex chromosomes (Ross et al. 2009; Peichel et al. 2020), our results show synapsis of the X and Y must be proceeding in a largely non-homologous fashion. Despite this, pairing is not delayed relative to autosomes.

The X chromosome undergoes synaptic adjustment during male meiosis

Among the fully paired X and Y chromosomes, two main conformations were identified based on the relative positions of the *Idh* markers. In one configuration, the *X-Idh* and *Y-Idh* markers were located further apart, but the Y-*Idh* marker was not at the end of the sex chromosome axis (20 out of 43 observed X/Y pairings; Fig. 1A). In this configuration, the SMC3 axis extended beyond the Y chromosome *Idh* signal. In the second configuration, the *X-Idh* marker was located in the middle and the *Y-Idh* marker was located at the end of the SMC3 axis (23 out of 43 observed X/Y pairings; Fig. 1B). These results are consistent with the shorter Y chromosome initially pairing with a longer X chromosome, followed by synaptic adjustment of the X to equalize the two SMC3 axes.

To test our hypothesis that synaptic adjustment was occurring between the non-homologously paired X and Y chromosomes, we first examined the overall timing of synaptic adjustment during prophase I. Synaptic adjustment does not occur until late pachytene (reviewed in Zickler and Kleckner 1999). Therefore, we predicted that the full adjustment configuration should be enriched in pachytene nuclei, relative to zygotene. We staged nuclei from four males to zygotene and pachytene (see methods). Consistent with synaptic adjustment, we found that the full synaptic adjustment configuration was enriched within pachytene nuclei, relative to zygotene (Fig. 2A, Fisher's exact test; P=0.007).

Second, we examined the size of chromatin loops organized around the SMC3 axis. The density of chromatin loops is highly conserved across taxa (Zickler and Kleckner 1999). Given constant DNA length, shorter synaptonemal complex axes result in chromatin loops that extend further from the axis, whereas longer axes result in loops that do not extend as far (Kleckner et al. 2003). For instance,



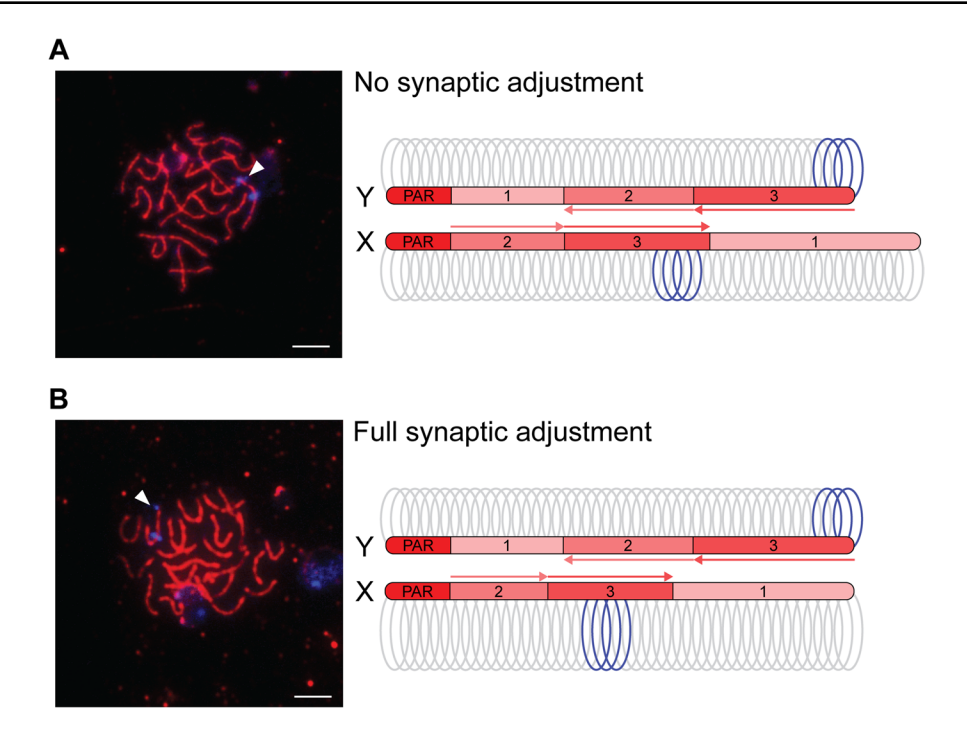


**Fig. 1** The threespine stickleback X and Y chromosomes undergo synaptic adjustment. Initially, the X chromosome synaptonemal complex axis extends beyond the length of the shorter Y chromosome (**A**). The sex chromosomes are marked with a fluorescent in situ hybridization DNA probe (*Idh*; blue). Due to chromosomal rearrangements between the X and Y, this marker is at the end of the Y chromosome, but it is located centrally within the X chromosome. Before synaptic adjustment, the axial element (SMC3; red) extends beyond the Y chromosome *Idh* marker (arrowhead). After synaptic adjustadjust-

differences in synaptonemal complex axis length between sexes of the same species result in a coordinated alteration in chromatin loop size (Tease and Hultén 2004; Gruhn et al. 2013). If synaptic adjustment was occurring, we predicted that the chromosome undergoing adjustment would exhibit a change in loop size between the no synaptic adjustment and the full synaptic adjustment conformations. We therefore measured the width of the X-Idh and Y-Idh FISH marker signals as a proxy for DNA loop size in the no adjustment (N=7) and full adjustment (N=10)conformations among pachytene nuclei. We found that while the Y-Idh loop size was the same in both conformations (Fig. 2B; Mann–Whitney U test; P=0.591), the X-Idh loop was wider in the full synaptic adjustment conformation (Fig. 2B; Mann-Whitney U Test; P=0.022). This indicates that synaptic adjustment occurs through shortening of the longer ment (**B**), this axis no longer extends beyond the Y chromosome *Idh* marker (arrowhead). The arrangements of the three main evolutionary strata on the X and Y chromosomes (1, 2, and 3; Peichel et al. 2020) are indicated on each axis, along with the pseudoautosomal region (PAR) where all crossing over occurs between the two chromosomes. The orientations of strata 2 and 3 are shown by arrows. The orientation of stratum 1 on the Y chromosome, relative to the X chromosome, cannot be determined due to the number of rearrangements in the region. Scale bar  $5 \, \mu m$ 

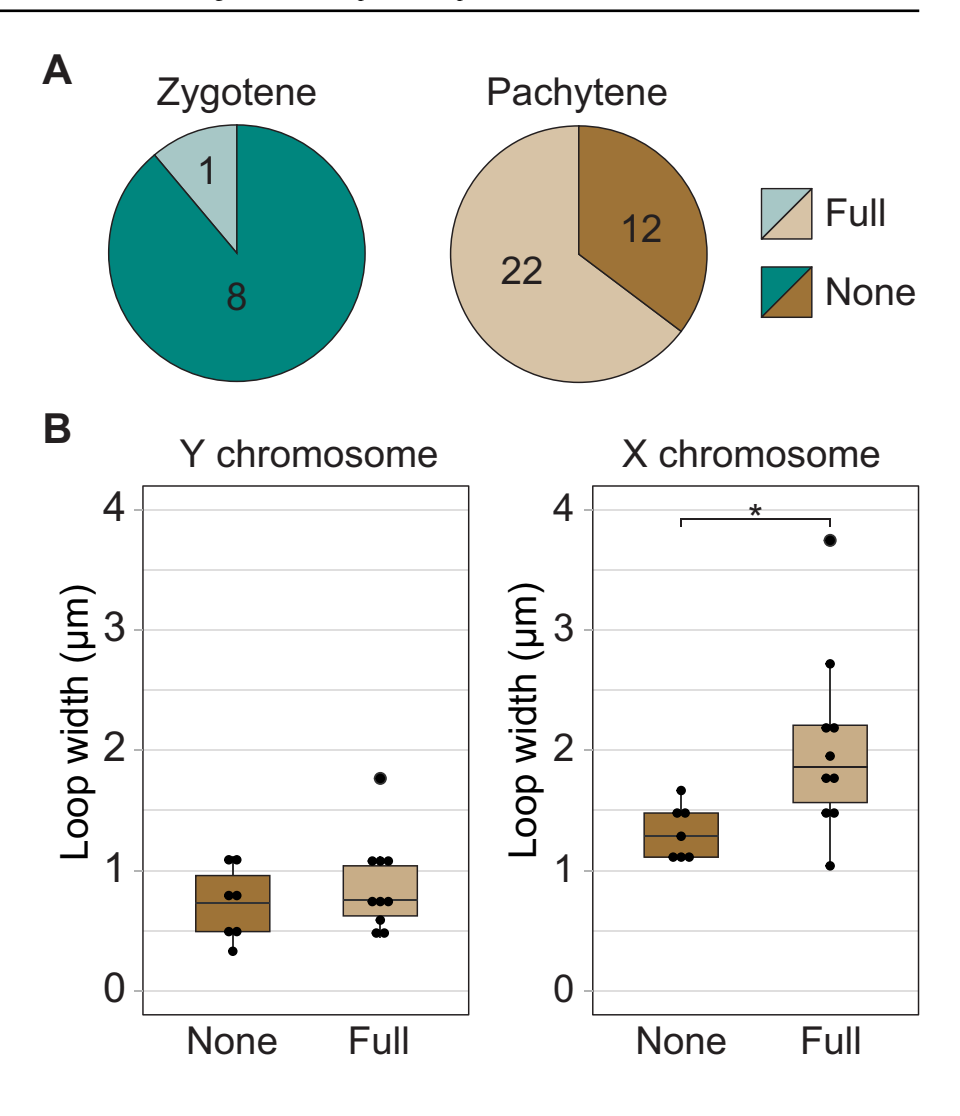
X chromosome axis. Our results are consistent with known patterns of synaptic adjustment on other chromosomes, where the longer axis shortens to match the length of the shorter axis (Zickler and Kleckner 1999; Lisachov et al. 2015).

DNA double-strand breaks form at a similar frequency on autosomes and sex chromosomes

To quantify the total number of DSBs throughout the genome, we counted the total number of RAD51 foci within meiotic nuclei (Fig. 3). RAD51 localizes to single-strand DNA at DSBs and has been used to cytologically visualize sites of DSB repair (Barlow et al. 1997; Fuente et al. 2007; Kauppi et al. 2011, 2012; Federici et al. 2015; Enguita-Marruedo et al. 2019). We found DSBs were at the highest density within leptotene (Fig. 4; N=34 nuclei; median:



**Fig. 2** The longer X chromosome axis contracts to adjust to the shorter Y chromosome axis as meiosis proceeds. There is a greater proportion of paired X and Y chromosomes that have undergone synaptic adjustment by pachytene (A; Fisher's exact test; P = 0.007). Due to the shortening axis, chromatin loops on the X chromosome are wider after full synaptic adjustment (B; Mann-Whitney *U* Test; P = 0.022). There was no change in chromatin loop width on the Y chromosome, indicating this chromosome axis is not undergoing adjustment. Chromatin loop width was measured at the Idh marker



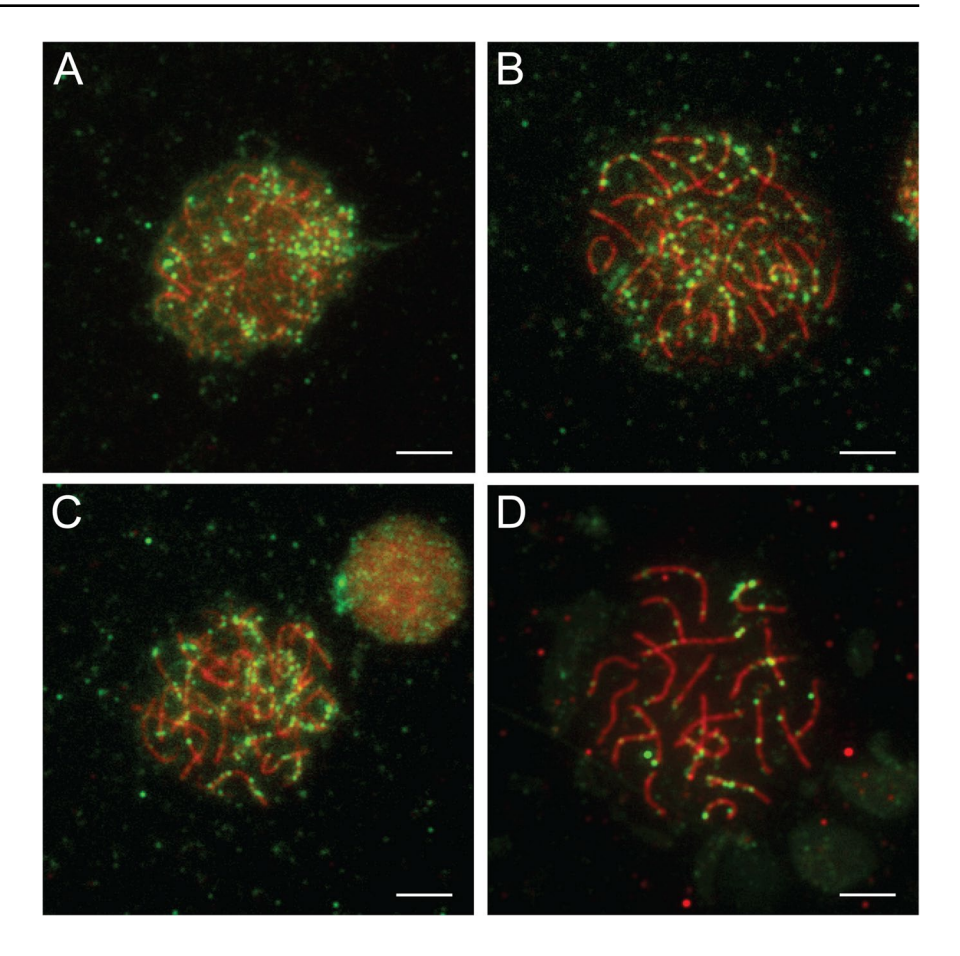
0.042 RAD51 foci/Mb). As prophase proceeds, double-strand breaks are repaired and the number of RAD51 foci decrease. Consistent with this, we observed a significant reduction of DSBs at each stage, decreasing as prophase proceeded (Fig. 4; zygotene N=53 nuclei; median: 0.024 RAD51 foci/Mb; pachytene N=34 nuclei; median: 0.005 RAD51 foci/Mb; Mann–Whitney U test; P<0.001 all pairwise comparisons, Bonferroni corrected for multiple comparisons).

Across the degenerated sex chromosomes of mammals, DSBs are suppressed and form at a lower density, relative to the autosomes (Lange et al. 2016). The DSBs that do form also exhibit delayed repair (Kauppi et al. 2011). It is unknown whether this difference in timing is characteristic of all heteromorphic sex

chromosomes, or whether less degenerated sex chromosomes may still exhibit DSB formation and repair similar to their ancestral autosome progenitors. We therefore tested whether the X and Y chromosomes of threespine stickleback fish exhibited any suppression of DSBs or whether they had counts that resembled that of autosomes. We focused on zygotene and pachytene stages when the X and Y chromosomes were fully synapsed. During zygotene, we found that the density of DSBs on the sex chromosomes was not significantly different from the density we observed on autosomes (Fig. 5; N=22; Mann–Whitney U test; P=0.327, Bonferroni corrected for multiple comparisons). Later in pachytene, the density of double-strand breaks was significantly lower on the sex chromosomes, compared to the autosomes (Fig. 5; N=23; Mann–Whitney U test;



Fig. 3 Double-strand breaks form throughout the genome. The greatest number of double-strand breaks occurs during leptotene (A) and decreases as meiosis proceeds through early zygotene (B), late zygotene (C), and pachytene (D). Double-strand breaks are immunolabeled against RAD51 (green). The synaptonemal complex axes are immunolabeled against the axial protein, SMC3 (red). Scale bar 5 µm



P=0.003, Bonferroni corrected for multiple comparisons). Combined, our results indicate that DSBs are not suppressed on the threespine stickleback X and Y chromosomes. In fact, the formation and repair of DSBs on the sex chromosomes coincides with the timing observed on autosomes.

Double-strand breaks on the sex chromosomes are not restricted to the pseudoautosomal region

DSBs occur at a higher density in the mammalian pseudoautosomal region compared to the unsynapsed region of the X and Y chromosomes (Lange et al. 2016). We therefore examined whether DSBs mainly occurred within the pseudoautosomal region of the threespine stickleback X and Y chromosomes or if DSBs also occurred across the remainder of the sex chromosomes where crossing over between the X and Y does not occur, despite being synapsed. We quantified the total number of DSBs in five equally sized regions across all autosomes and the

sex chromosomes. The Y chromosome Idh marker is located at the opposite end of the chromosome from the pseudoautosomal region, which allowed us to cytologically separate the sex-determining region from the pseudoautosomal region. On autosomes, we found the total number of DSBs was highest at the ends of the chromosomes (Fig. 6; N=420 autosomes). On the sex chromosomes, we observed a pattern of DSB formation that closely resembled that of the autosomes. We found most of the DSBs were located at the ends of the sex chromosomes (Fig. 6; N=47 X/Y chromosomes). Importantly, this includes the end of the chromosome opposite from the pseudoautosomal region, which does not undergo crossing over during meiosis. In addition, we also observed DSBs throughout the central part of the sex chromosomes that also do not undergo crossing over. Although we could not distinguish whether DSBs formed more often on the X or Y chromosome at this resolution, our results clearly indicated DSBs do occur throughout the sex-determining region.



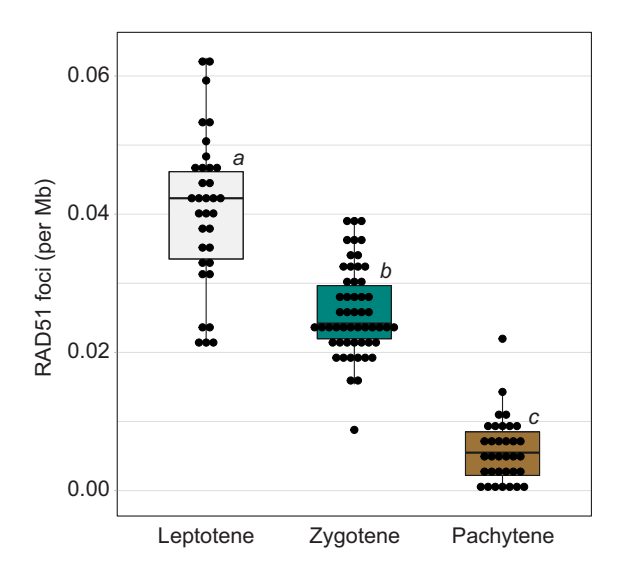


**Fig. 4** Double-strand breaks throughout the genome are repaired as meiosis proceeds. The highest density of RAD51 foci throughout the genome was found during leptotene. The lowest density was observed during pachytene. Stages of meiosis significantly different from one another are indicated by a, b, and c (Mann–Whitney U test; P < 0.05; Bonferroni corrected for multiple comparisons)

#### Discussion

The lack of sequence homology between heteromorphic sex chromosomes leads to pairing challenges during meiosis. The pairing of homologs requires engagement of single-strand DNA at DSBs between homologs (Baudat et al. 2000; Romanienko and Camerini-Otero 2000). In mammals, this occurs within the pseudoautosomal region (Solari 1974). More extensive pairing outside of the pseudoautosomal region has been observed in a subset of meiocytes (Solari 1970; Tres 1977; Chandley et al. 1984), but stable pairing is largely restricted to this short stretch of sequence homology. Unlike mammals, we observed complete pairing of the threespine stickleback heteromorphic X and Y chromosomes in nearly all meiocytes, indicating stable pairing is achieved along the entire length of the X and Y chromosomes. This pattern matches earlier work using electron microscopy that noted all chromosomes fully pair (Cuñado et al. 2002). Full pairing is observed among other teleost species and does not seem to be strongly correlated with overall structural divergence between the X and Y. For instance, the *Poecilia reticulata* guppy Y chromosome fully pairs with the X chromosome

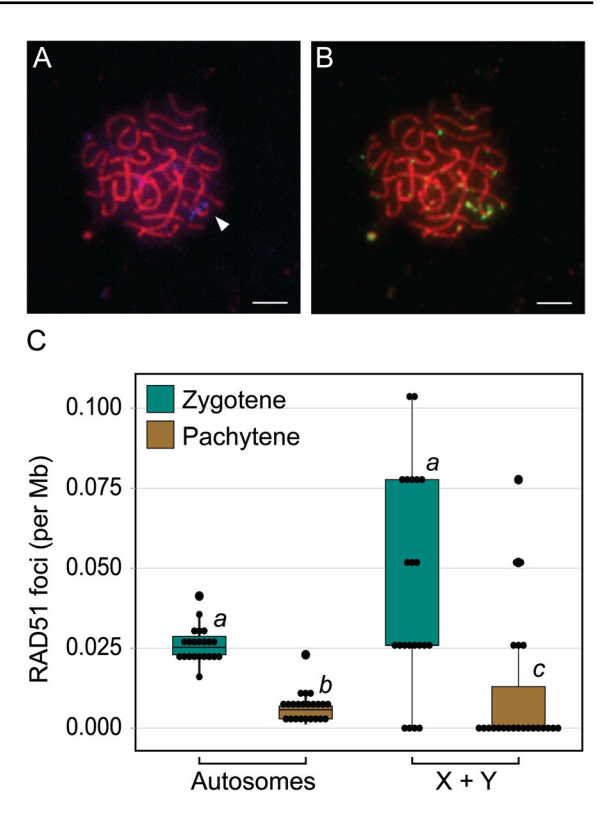


**Fig. 5** The threespine stickleback sex chromosomes have a similar density of double-strand breaks as autosomes. Meiocytes at pachytene were labeled with *Idh* to distinguish the sex chromosomes (blue; arrowhead) from the autosomes (**A**). RAD51 foci (green) were counted on all chromosomes (**B**). Autosomes and sex chromosomes have an indistinguishable density of RAD51 foci at zygotene (**C**). The density of RAD51 foci is lower on sex chromosomes compared to autosomes at pachytene, indicating breaks may actually repair faster. Groups significantly different from one another are indicated by a, b, and c (Mann–Whitney U test; P<0.05; Bonferroni corrected for multiple comparisons). Scale bar 5 μm

(Lisachov et al. 2015). In this species, homology between the X and Y chromosomes is high. The Y chromosome does not exhibit extensive sequence degeneration and does not contain any structural rearrangements (Wright et al. 2017; Darolti et al. 2020; Charlesworth et al. 2021). In fact, rare crossover events between the X and Y are still observed in the sex determination region (Bergero et al. 2019), indicating DSBs can be repaired using inter-gametolog templates. Full pairing is also observed in some meiocytes of the swamp guppy, *Micropoecilia picta*. Unlike *P. reticulata*, the Y chromosome of this species exhibits a substantial size reduction and high heterochromatin content, relative to the X chromosome



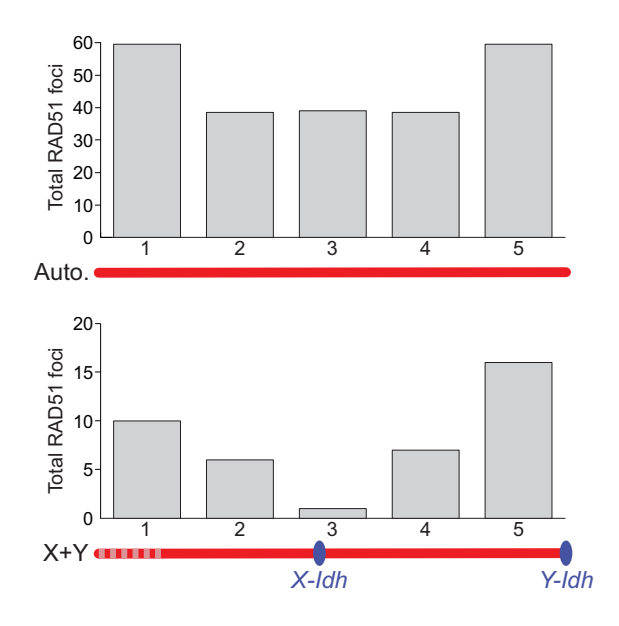


**Fig. 6** RAD51 foci occur most frequently at the terminal ends of chromosomes on both the autosomes and the sex chromosomes. Each SMC3 axis was divided into five equally sized segments and RAD51 foci were counted within each segment. The pseudoautosomal region (vertical lines) is indicated and is located at the end opposite of the terminal *Idh* marker (blue) on the paired X and Y chromosome

(Nanda et al. 2022). Full pairing is also observed between the X and Y chromosomes of the Nile tilapia (*Oreochromis niloticus*) among a majority of meiocytes (Carrasco et al. 1999). In this species, there is a sex determination region that is approximately 23% of the chromosome length (Gammerdinger et al. 2014; Conte et al. 2017).

It is unclear how the threespine stickleback X and Y chromosomes achieve full pairing during meiosis with extensive degeneration outside of the pseudoautosomal region in addition to major inversions (Ross and Peichel 2008; Peichel et al. 2020). There are no colinear regions of sequence homology between the X and Y within the sex determination region (Fig. 1). In birds, full heterologous pairing occurs between the Z chromosome and the ancient, degenerated W chromosome and may be facilitated by regions of repetitive microhomology between the two gametologs (Guioli et al. 2012). A similar mechanism may be operating in threespine stickleback. Transposable elements have accumulated throughout the non-recombining region of the threespine stickleback Y chromosome and are also at a higher density throughout the X chromosome (Peichel et al. 2020). Additional work will be necessary to determine if pairing of the threespine stickleback sex chromosomes is facilitated by establishing interaxis bridges at DSBs that form around repetitive elements. Knocking out *Spo11* would provide insight into whether homology-based DSB repair is required for pairing and synapsis of the sex chromosomes (Baudat et al. 2000; Romanienko and Camerini-Otero 2000).

Full pairing of the threespine stickleback X and Y is achieved through synaptic adjustment of the X chromosome to match the length of the shorter Y chromosome. We did not observe inversion loops during early meiosis that would suggest pairing initially begins in a homologous fashion, as observed in mouse inversion heterozygotes. In mice, inversion loops later undergo synaptic adjustment by pachytene to form a linear synaptonemal complex (Moses et al. 1982; Zickler and Kleckner 1999). Instead, the X and Y paired nonhomologously throughout the non-crossover region. Synaptic adjustment only occurred to compensate for the length difference between the X and Y. It remains unknown whether synaptic adjustment relies on DNAbased or protein-based signals, but it has been postulated that one mechanism may be to match up telomeres between paired homologs (MacQueen et al. 2005). Synaptic adjustment of sex chromosomes has been documented in other teleost species (Carrasco et al. 1999; Traut and Winking 2001) and the chicken (Solari 1992), preventing any regions of the sex chromosomes from remaining unsynapsed. Asynapsis of sex chromosomes leads to transcriptional silencing of the chromosomes during pachytene (meiotic sex chromosome inactivation) (Turner et al. 2006; Turner 2007). Indeed, in chickens, there is no evidence of meiotic sex chromosome inactivation (Guioli et al. 2012), where there is synaptic adjustment. We predict that synaptic adjustment in threespine stickleback fish will also prevent meiotic sex chromosome inactivation of the sex chromosomes during pachytene. Single-cell RNA-seq will be a useful approach to test this hypothesis by characterizing transcription of the sex chromosomes relative to the autosomes at each stage of meiosis (Lukassen et al. 2018).

DSBs form on the threespine stickleback sex chromosomes at a density similar to autosomes. This result stands in stark contrast to the mammalian sex chromosomes, where DSBs are suppressed outside of the pseudoautosomal region (Moens et al. 1997;



Lange et al. 2016). The resolution of our experiments does not allow us to accurately place DSBs inside or outside of the pseudoautosomal region when they are near the border. However, over half of the DSBs we detected on the sex chromosomes were far from the border, at the end opposite from the pseudoautosomal region. Our results show that more recently derived sex chromosomes can accumulate DSBs with distributions that more closely resemble that of autosomes, with DSBs enriched at chromosome ends. Across taxa, males often have recombination rates that are higher towards chromosome ends (reviewed in Sardell and Kirkpatrick 2019). The RAD51 distribution we found matches recombination rates estimated through genetic maps in threespine stickleback fish, where males have crossover frequencies higher at chromosome ends, relative to females (Sardell et al. 2018). In humans, DSBs also occur more frequently at the end of chromosomes, suggesting DSB initiation could be the main factor that increases recombination rate within these regions (Pratto et al. 2014).

During meiosis, there is a strong bias towards using the homolog as a repair template (reviewed in Lao and Hunter 2010). For highly degenerate sex chromosomes, the lack of homology between gametologs leads to a delay in repair until late pachytene (Moens et al. 1997; Pratto et al. 2014; Federici et al. 2015; Lange et al. 2016) when constraints against other repair options are lifted (non-homologous end joining and homologous recombination with the sister chromatid). Components of the non-homologous end joining pathway are enriched around the mouse X and Y chromosomes during pachytene (Goedecke et al. 1999; Enguita-Marruedo et al. 2019), which resembles somatic-like DNA repair, rather than meiotic-like repair that is biased towards recombination with the homolog (Enguita-Marruedo et al. 2019). Unlike mammals, we did not find delayed DSB repair on the threespine stickleback X and Y chromosomes. The breaks repair at the same rate as DSBs located on the autosomes. This supports a model where DSBs on more recently derived sex chromosomes can be repaired using inter-gametolog templates when the bias against sister chromatid repair and non-homologous end joining is operating. The early DSB repair we observed is consistent with single-end invasion processes and non-crossover exchange during zygotene (Hunter and Kleckner 2001). We postulate that this is occurring at sites with repetitive elements that share substantial sequence identity. Once these interactions between the X and Y are resolved, this would permit reconfiguration of the synaptonemal complex to adjust for the length difference between the X and Y by pachytene. Non-crossover gene conversion has been observed between X and Y chromosomes of other species, including the ancient mammalian sex chromosomes (Rosser et al. 2009; Trombetta et al. 2010, 2014). These repair events can involve sequence exchange between transposable elements (Trombetta et al. 2016). This process may help purge deleterious mutations from the Y chromosome (Marais et al. 2010; Connallon and Clark 2010; Sakamoto and Innan 2021). With a similar density of DSBs on the sex chromosomes as the autosomes, our results suggest gene conversion may occur at a higher rate on more recently derived sex chromosomes. Additional work needs to focus on determining what DNA templates are primarily used to repair DSBs in the threespine stickleback sex-determining region.

Our work has revealed that recently derived sex chromosomes behave more like their ancestral autosomal progenitors during meiosis. The rates of pairing, DSB formation, and DSB repair on sex chromosomes were indistinguishable from the autosomes. Stickleback fish offer a powerful model system to explore how the meiotic behavior of sex chromosomes varies at different evolutionary scales. In addition to threespine stickleback fish, there are several closely related species with independently derived sex chromosomes of various ages (Ross et al. 2009). Comparative molecular cytogenetic approaches across these species will help reveal the generality of these processes over different time scales and will provide important insights into whether gene conversion between the X and Y could play a substantial role in the sequence evolution of newly evolving sex chromosomes.

Acknowledgements The authors thank Shaugnessy McCann, Jackie Cory, Jim Cory, Damean McCann, and Bill Frothingham for assistance collecting threespine stickleback fish. Kelly Dawe, Beth Dumont, and Kyle Swentowsky provided assistance in troubleshooting and useful discussions of our results. Brittany Dorsey helped count RAD51 foci.

**Author contribution** M.A.W. and S.N. conceived and designed the study. S.N., L.A.W., and M.K.F. performed the research. S.N. and M.A.W. analyzed the data. S.N. and M.A.W. wrote the paper.



**Funding** This work was supported by the National Science Foundation MCB 1943283 to M.A.W.

#### **Declarations**

Conflict of interest The authors declare no competing interests

#### References

- Ashley T, Plug AW, Xu J et al (1995) Dynamic changes in Rad51 distribution on chromatin during meiosis in male and female vertebrates. Chromosoma 104:19–28. https://doi.org/10.1007/bf00352222
- Bachtrog D (2013) Y-chromosome evolution: emerging insights into processes of Y-chromosome degeneration. Nat Rev Genet 14:113–124. https://doi.org/10.1038/nrg33
- Barlow AL, Benson FE, West SC, Hultén MA (1997) Distribution of the Rad51 recombinase in human and mouse spermatocytes. Embo J 16:5207–5215. https://doi.org/10.1093/emboi/16.17.5207
- Baudat F, Manova K, Yuen JP et al (2000) Chromosome synapsis defects and sexually dimorphic meiotic progression in mice lacking Spo11. Mol Cell 6:989–998. https://doi.org/10.1016/s1097-2765(00)00098-8
- Bellott DW, Hughes JF, Skaletsky H et al (2014) Mammalian Y chromosomes retain widely expressed dosage-sensitive regulators. Nature 508:494–499. https://doi.org/10.1038/nature13206
- Bergero R, Gardner J, Bader B et al (2019) Exaggerated heterochiasmy in a fish with sex-linked male coloration polymorphisms. Proc National Acad Sci 116:6924–6931. https://doi.org/10.1073/pnas.1818486116
- Blokhina YP, Nguyen AD, Draper BW, Burgess SM (2019)
  The telomere bouquet is a hub where meiotic double-strand breaks, synapsis, and stable homolog juxtaposition are coordinated in the zebrafish. Danio Rerio Plos Genet 15:e1007730. https://doi.org/10.1371/journal.pgen.1007730
- Borg B (1982) Seasonal effects of photoperiod and temperature on spermatogenesis and male secondary sexual characters in the three-spined stickleback, Gasterosteus aculeatus L. Can J Zool 60:3377–3386
- Borodin PM, Basheva EA, Torgasheva AA et al (2011) Multiple independent evolutionary losses of XY pairing at meiosis in the grey voles. Chromosome Res 20:259–268. https://doi.org/10.1007/s10577-011-9261-0
- Burgoyne PS (1982) Genetic homology and crossing over in the X and Y chromosomes of Mammals. Hum Genet 61:85–90
- Carrasco LAP, Penman DJ, Bromage N (1999) Evidence for the presence of sex chromosomes in the Nile tilapia (Oreochromis niloticus) from synaptonemal complex analysis of XX, XY and YY genotypes. Aquaculture 173:207–218. https://doi.org/10.1016/s0044-8486(98)00488-8
- Chandley AC, Goetz P, Hargreave TB et al (1984) On the nature and extent of XY pairing at meiotic prophase in

- man. Cytogenet Genome Res 38:241–247. https://doi.org/10.1159/000132070
- Charlesworth D, Bergero R, Graham C et al (2021) How did the guppy Y chromosome evolve? Plos Genet 17:e1009704. https://doi.org/10.1371/journal.pgen.1009704
- Checchi PM, Engebrecht J (2011) Heteromorphic sex chromosomes: navigating meiosis without a homologous partner.

  Mol Reprod Dev 78:623–632. https://doi.org/10.1002/mrd.21369
- Connallon T, Clark AG (2010) Gene duplication, gene conversion and the evolution of the Y chromosome. Genetics 186:277–286. https://doi.org/10.1534/genetics.110.116756
- Conte MA, Gammerdinger WJ, Bartie KL et al (2017) A high quality assembly of the Nile Tilapia (Oreochromis niloticus) genome reveals the structure of two sex determination regions. BMC Genomics 18:341. https://doi.org/10.1186/s12864-017-3723-5
- Cortez D, Cortez D, Marin R et al (2014) Origins and functional evolution of Y chromosomes across mammals. Nature 508:488–493. https://doi.org/10.1038/nature13151
- Craig-Bennett A (1931) The reproductive cycle of the three-spined stickleback, Gasterosteus aculeatus. Linn Phil Trans Roy Soc B 219:197–279. https://doi.org/10.2307/92176
- Cuñado N, Barrios J, Miguel ES et al (2002) Synaptonemal complex analysis in oocytes and spermatocytes of threespine stickleback Gasterosteus aculeatus (Teleostei, Gasterosteidae). Genetica 114:53–56. https://doi.org/10.1023/a: 1014685114092
- Darolti I, Wright AE, Mank JE (2020) Guppy Y chromosome integrity maintained by incomplete recombination suppression. Genome Biol Evol 12:evaa099. https://doi.org/ 10.1093/gbe/evaa099
- Dawe RK, Lowry EG, Gent JI et al (2018) A kinesin-14 motor activates neocentromeres to promote meiotic drive in maize. Cell 173:839-850.e18. https://doi.org/10.1016/j. cell.2018.03.009
- Dumont BL, Payseur BA (2011) Genetic analysis of genomescale recombination rate evolution in house mice. PLoS Genet 7:e1002116. https://doi.org/10.1371/journal.pgen. 1002116
- Dumont BL, Williams CL, Ng BL et al (2018) Relationship between sequence homology, genome architecture, and meiotic behavior of the sex chromosomes in North American voles. Genetics 210:83–97. https://doi.org/10.1534/genetics.118.301182
- Enguita-Marruedo A, Martín-Ruiz M, García E et al (2019)
  Transition from a meiotic to a somatic-like DNA damage response during the pachytene stage in mouse meiosis.
  Plos Genet 15:e1007439. https://doi.org/10.1371/journal.pgen.1007439
- Federici F, Mulugeta E, Schoenmakers S et al (2015) Incomplete meiotic sex chromosome inactivation in the domestic dog. BMC Genomics 16:291. https://doi.org/10.1186/s12864-015-1501-9
- de la Fuente R, Parra MT, Viera A et al (2007) Meiotic pairing and segregation of achiasmate sex chromosomes in eutherian mammals: the role of SYCP3 protein. Plos Genet 3:e198. https://doi.org/10.1371/journal.pgen.0030198



- de la Fuente R, Sánchez A, Marchal JA et al (2012) A synaptonemal complex-derived mechanism for meiotic segregation precedes the evolutionary loss of homology between sex chromosomes in arvicolid mammals. Chromosoma 121:433–446. https://doi.org/10.1007/s00412-012-0374-9
- Gammerdinger WJ, Conte MA, Acquah EA et al (2014) Structure and decay of a proto-Y region in tilapia, Oreochromis niloticus. Bmc Genomics 15:975. https://doi.org/10.1186/1471-2164-15-975
- Goedecke W, Eijpe M, Offenberg HH et al (1999) Mre11 and Ku70 interact in somatic cells, but are differentially expressed in early meiosis. Nat Genet 23:194–198. https://doi.org/10.1038/13821
- Grelon M, Vezon D, Gendrot G, Pelletier G (2001) AtSPO11-1 is necessary for efficient meiotic recombination in plants. EMBO J 20:589–600
- Gruhn JR, Rubio C, Broman KW et al (2013) Cytological studies of human meiosis: sex-specific differences in recombination originate at, or prior to, establishment of double-strand breaks. PLoS ONE 8:e85075. https://doi.org/10.1371/journal.pone.0085075
- Guioli S, Lovell-Badge R, Turner JMA (2012) Error-prone ZW pairing and no evidence for meiotic sex chromosome inactivation in the chicken germ line. Plos Genet 8:e1002560. https://doi.org/10.1371/journal.pgen.1002560
- Hassold T, Hunt P (2001) To err (meiotically) is human: the genesis of human aneuploidy. Nat Rev Genet 2:280–291. https://doi.org/10.1038/35066065
- Hassold TJ, Sherman SL, Pettay D et al (1991) XY chromosome nondisjunction in man is associated with diminished recombination in the pseudoautosomal region. Am J Hum Genet 49:253–260
- Hunter N, Kleckner N (2001) The single-end invasion an asymmetric intermediate at the double-strand break to double-holliday junction transition of meiotic recombination. Cell 106:59–70. https://doi.org/10.1016/s0092-8674(01) 00430-5
- Inagaki A, Schoenmakers S, Baarends WM (2010) DNA double strand break repair, chromosome synapsis and transcriptional silencing in meiosis. Epigenetics 5:255–266. https://doi.org/10.4161/epi.5.4.11518
- Kauppi L, Barchi M, Baudat F et al (2011) Distinct properties of the XY pseudoautosomal region crucial for male meiosis. Science 331:916–920. https://doi.org/10.1126/science. 1195774
- Kauppi L, Jasin M, Keeney S (2012) The tricky path to recombining X and Y chromosomes in meiosis. Ann Ny Acad Sci 1267:18–23. https://doi.org/10.1111/j.1749-6632. 2012.06593.x
- Kleckner N, Storlazzi A, Zickler D (2003) Coordinate variation in meiotic pachytene SC length and total crossover/chiasma frequency under conditions of constant DNA length. Trends Genet 19:623–628. https://doi.org/10.1016/j.tig. 2003.09.004
- Lange J, Yamada S, Tischfield SE et al (2016) The landscape of mouse meiotic double-strand break formation, processing, and repair. Cell 167:695–708. https://doi.org/10.1016/j.cell.2016.09.035
- Lao JP, Hunter N (2010) Trying to avoid your sister. Plos Biol 8:e1000519. https://doi.org/10.1371/journal.pbio.1000519

- Lisachov AP, Zadesenets KS, Rubtsov NB, Borodin PM (2015) Sex chromosome synapsis and recombination in male guppies. Zebrafish 12:174–180. https://doi.org/10.1089/ zeb.2014.1000
- Lu L-Y, Yu X (2015) Double-strand break repair on sex chromosomes: challenges during male meiotic prophase. Cell Cycle 14:516–525. https://doi.org/10.1080/15384101. 2014.998070
- Lukassen S, Bosch E, Ekici AB, Winterpacht A (2018) Characterization of germ cell differentiation in the male mouse through single-cell RNA sequencing. Sci Rep 8:6521. https://doi.org/10.1038/s41598-018-24725-0
- MacQueen AJ, Phillips CM, Bhalla N et al (2005) Chromosome sites play dual roles to establish homologous synapsis during meiosis in C. elegans. Cell 123:1037–1050. https://doi.org/10.1016/j.cell.2005.09.034
- Mahadevaiah SK, Turner JMA, Baudat F et al (2001) Recombinational DNA double-strand breaks in mice precede synapsis. Nat Genet 27:271–276. https://doi.org/10.1038/85830
- Marais GAB, Marais GAB, Campos PRA et al (2010) Can intra-Y gene conversion oppose the degeneration of the human Y chromosome? A simulation study. Genome Biol Evol 2:347–357. https://doi.org/10.1093/gbe/evq026
- Moens PB, Chen DJ, Shen Z et al (1997) Rad51 immunocytology in rat and mouse spermatocytes and oocytes. Chromosoma 106:207–215. https://doi.org/10.1007/s0041 20050241
- Moses MJ, Poorman PA, Roderick TH, Davisson MT (1982) Synaptonemal complex analysis of mouse chromosomal rearrangements. IV. Synapsis and synaptic adjustment in two paracentric inversions. Chromosoma 84:457–474. https://doi.org/10.1007/bf00292848
- Naftaly AS, Pau S, White MA (2021) Long-read RNA sequencing reveals widespread sex-specific alternative splicing in threespine stickleback fish. Genome Res 31:1486–1497. https://doi.org/10.1101/gr.274282.120
- Nanda I, Schories S, Simeonov I et al (2022) Evolution of the degenerated Y-chromosome of the swamp guppy. Micropoecilia Picta Cells 11:1118. https://doi.org/10. 3390/cells11071118
- Page J, Berríos S, Parra MT et al (2005) The program of sex chromosome pairing in meiosis is highly conserved across marsupial species implications for sex chromosome evolution. Genetics 170:793–799. https://doi.org/10.1534/genet ics.104.039073
- Page J, de la Fuente R, Gómez R et al (2006) Sex chromosomes, synapsis, and cohesins: a complex affair. Chromosoma 115:250–259. https://doi.org/10.1007/s00412-006-0059-3
- Peichel CL, McCann SR, Ross JA et al (2020) Assembly of the threespine stickleback Y chromosome reveals convergent signatures of sex chromosome evolution. Genome Biol 21:177. https://doi.org/10.1186/s13059-020-02097-x
- Peichel CL, Ross JA, Matson CK et al (2004) the master sexdetermination locus in threespine sticklebacks is on a nascent Y chromosome. Curr Biol 14:1416–1424. https://doi. org/10.1016/j.cub.2004.08.030
- Pratto F, Brick K, Khil P et al (2014) Recombination initiation maps of individual human genomes. Science 346:1256442. https://doi.org/10.1126/science.1256442



- Rasmussen SW, Holm PB (1978) Human meiosis II. Chromosome pairing and recombination nodules in human spermatocytes. Carlsberg Res Commun 43:275. https://doi.org/10.1007/bf02906106
- Roesti M, Moser D, Berner D (2013) Recombination in the threespine stickleback genome-patterns and consequences. Mol Ecol 22:3014–3027. https://doi.org/10. 1111/mec.12322
- Romanienko PJ, Camerini-Otero RD (2000) The mouse Spo11 gene is required for meiotic chromosome synapsis. Mol Cell 6:975–987. https://doi.org/10.1016/s1097-2765(00) 00097-6
- Ross JA, Peichel CL (2008) Molecular cytogenetic evidence of rearrangements on the Y chromosome of the threespine stickleback fish. Genetics 179:2173–2182. https://doi.org/10.1534/genetics.108.088559
- Ross JA, Urton JR, Boland J et al (2009) Turnover of sex chromosomes in the stickleback fishes (Gasterosteidae). PLOS Genet 5:e1000391. https://doi.org/10.1371/journal.pgen. 1000391
- Rosser ZH, Balaresque P, Jobling MA (2009) Gene conversion between the X chromosome and the male-specific region of the Y chromosome at a translocation hotspot. Am J Hum Genetics 85:130–134. https://doi.org/10.1016/j.ajhg. 2009.06.009
- Rouyer F, Simmler M-C, Johnsson C et al (1986) A gradient of sex linkage in the pseudoautosomal region of the human sex chromosomes. Nature 319:291–295. https://doi.org/10.1038/319291a0
- Sakamoto T, Innan H (2021) Muller's ratchet of the Y chromosome with gene conversion. Genetics 220:iyab204. https://doi.org/10.1093/genetics/iyab204
- Sardell JM, Cheng C, Dagilis AJ et al (2018) Sex differences in recombination in sticklebacks. G3 8:1971–1983. https:// doi.org/10.1534/g3.118.200166
- Sardell JM, Kirkpatrick M (2019) Sex differences in the recombination landscape. Am Nat 195:361–379. https://doi.org/10.1086/704943
- Schoenmakers S, Wassenaar E, Hoogerbrugge JW et al (2009) Female meiotic sex chromosome inactivation in chicken. Plos Genet 5:e1000466. https://doi.org/10.1371/journal.pgen.1000466
- Solari AJ (1992) Equalization of Z and W axes in chicken and quail oocytes. Cytogenet Genome Res 59:52–56. https://doi.org/10.1159/000133199
- Solari AJ (1974) The behavior of the XY pair in mammals. Int Rev Cytol 38:273–317. https://doi.org/10.1016/s0074-7696(08)60928-6
- Solari AJ (1970) The spatial relationship of the X and Y chromosomes during meiotic prophase in mouse spermatocytes. Chromosoma 29:217–236. https://doi.org/10.1007/bf00326080

- Soriano P, Keitges EA, Schorderet DF et al (1987) High rate of recombination and double crossovers in the mouse pseudoautosomal region during male meiosis. Proc National Acad Sci 84:7218–7220. https://doi.org/10.1073/pnas.84. 20.7218
- Tease C, Hultén MA (2004) Inter-sex variation in synaptonemal complex lengths largely determine the different recombination rates in male and female germ cells. Cytogenet Genome Res 107:208–215. https://doi.org/10.1159/000080599
- Traut W, Winking H (2001) Meiotic chromosomes and stages of sex chromosome evolution in fish: zebrafish, platyfish and guppy. Chromosome Res 9:659–672. https://doi.org/10.1023/a:1012956324417
- Tres LL (1977) Extensive pairing of the XY bivalent in mouse spermatocytes as visualized by whole-mount electron microscopy. J Cell Sci 25:1–15
- Trombetta B, Cruciani F, Underhill PA et al (2010) Footprints of X-to-Y gene conversion in recent human evolution. Mol Biol Evol 27:714–725. https://doi.org/10.1093/molbev/msp231
- Trombetta B, Fantini G, D'Atanasio E et al (2016) Evidence of extensive non-allelic gene conversion among LTR elements in the human genome. Sci Rep 6:28710. https://doi.org/10.1038/srep28710
- Trombetta B, Sellitto D, Scozzari R, Cruciani F (2014) Interand intraspecies phylogenetic analyses reveal extensive X-Y gene conversion in the evolution of gametologous sequences of human sex chromosomes. Mol Biol Evol 31:2108–2123. https://doi.org/10.1093/molbev/msu155
- Turner JMA (2007) Meiotic sex chromosome inactivation.

  Development (Cambridge, England) 134:1823–1831.

  https://doi.org/10.1242/dev.000018
- Turner JMA, Mahadevaiah SK, Ellis PJI et al (2006) Pachytene asynapsis drives meiotic sex chromosome inactivation and leads to substantial postmeiotic repression in spermatids. Dev Cell 10:521–529. https://doi.org/10.1016/j.devcel. 2006.02.009
- Wright AE, Darolti I, Bloch NI et al (2017) Convergent recombination suppression suggests role of sexual selection in guppy sex chromosome formation. Nat Commun 8:14251. https://doi.org/10.1038/ncomms14251
- Zhou Q, Zhang J, Bachtrog D et al (2014) Complex evolutionary trajectories of sex chromosomes across bird taxa. Science 346:1246338. https://doi.org/10.1126/science.1246338
- Zickler D, Kleckner N (1999) Meiotic chromosomes: integrating structure and function. Annu Rev Genet 33:603–754. https://doi.org/10.1146/annurev.genet.33.1.603

**Publisher's note** Springer Nature remains neutral with regard to jurisdictional claims in published maps and institutional affiliations.

